Zeta Potential in Intact Carbonates at Reservoir Conditions and its Impact on Oil Recovery During Controlled Salinity Waterflooding.

Harry Collini[1], Shuai Li[1,2], Matthew D. Jackson[1], Nicolas Agenet[3], Bilal Rashid[4], John Couves[4]

1. **Department of Earth Science & Engineering, Imperial College London, UK**
2. **Now at Hubei Subsurface Multi-scale Imaging Key Laboratory, Institute of Geophysics and Geomatics, China University of Geosciences, Wuhan 430074, China.**
3. **TOTAL, Centre Scientifique et Technique Jean Féger, Avenue Larribau, 64000 Pau, France.**
4. **BP Exploration, Subsurface Technical Centre, Sunbury-upon-Thames, UK**

Abstract

It is well known that oil recovery from carbonate reservoirs can be increased by modifying the injected brine composition in a process 'controlled salinity water-flooding' (CSW). However, the mineral- to pore-scale processes responsible for improved oil recovery (IOR) during CSW remain ambiguous and there is no method to predict the optimum CSW composition for a given crude-oil-brine rock system. Here we report the first integrated experimental measurements of zeta potential and IOR during CSW obtained at reservoir conditions. The zeta potential is a measure of the electrical potential at mineral-brine and oil-brine interfaces and controls the electrostatic forces acting between these interfaces.

We find that the measured zeta potential in clean samples saturated with formation brine is typically positive and becomes more negative with brine dilution irrespective of temperature. After aging and wettability alteration, the zeta potential changes and we suggest a more positive zeta potential indicates a positive zeta potential at the oil-brine interface and vice-versa. Injecting low salinity brine yields IOR when the oil-brine zeta potential is identified to be negative, but no response when it is identified to be positive, consistent with the hypothesis that IOR during CSW is caused by an increase in the repulsive electrostatic force acting between mineral-brine and oil-brine interfaces. We suggest that the optimum brine composition for IOR during CSW should be chosen to yield the largest change in zeta potential at the mineral-brine interface with opposing polarity to the oil-brine interface and can be determined using the experimental method reported here.

Introduction

Carbonate reservoirs contain a substantial amount of the world's oil reserves, but recoveries are typically low (<40%) [1]. Laboratory experiments and field trials have shown that improved oil recovery (IOR) from carbonate reservoirs can be obtained by modifying the injected brine composition in a process termed controlled salinity water-flooding (CSW) [2-6]. CSW is appealing due to its relative simplicity, low cost, easy implementation and avoidance of complex engineering or chemical additives such as polymers or surfactants. Typically, the injected brine is of lower salinity than the naturally present formation brine; it may comprise seawater and/or diluted seawater, or low-salinity water with a specific ionic composition. There has been significant research to understand the underlying mechanisms controlling CSW and several have been proposed, including calcite dissolution [7], the presence of sulphate (and/or dissolution of anhydrite) [3] and changes in the carbonate mineral surface charge [8, 9]. However, no one mechanism has yet been shown to yield IOR in all crude oil/brine/rock (COBR) systems;

49 moreover, most fail to explain why published results (and many more unpublished) show no IOR
50 with dilution of the injection brine [3, 5]. The mineral- to pore- scale processes responsible for
51 improved recovery during CSW remain ambiguous and there is no definitive method to predict
52 whether a given COBR system will respond to a controlled salinity water flood, or to identify the
53 optimum injection brine composition to maximize IOR.
54
55 One common theme across the various mineral- to pore- scale mechanisms that have been
56 proposed to underpin CSW is that they are associated with changes in the zeta potential at the
57 carbonate mineral-brine interface (e.g. [3, 7-9]) The zeta potential is a measure of the electrical
58 potential at the interface and is widely measured in colloid and interface science [10]. Numerous
59 studies have reported measurements of the zeta potential on both natural and artificial
60 calcite/carbonate surfaces in contact with electrolytes with a range of composition and total ionic
61 strength. A recent review was provided by [11], who concluded that the zeta potential of calcium
62 carbonate mineral surfaces is primarily controlled by adsorption of lattice species Ca^{2+} and Mg^{2+}
63 (e.g. Figure *1* (a)). Decreasing the concentration of these divalent ions yields an increasingly
64 negative zeta potential, and both behave identically within experimental error at laboratory
65 conditions [11, 12]. The total ionic strength of the brine also affects the magnitude of the zeta
66 potential, because it controls the thickness of the diffuse part of the electrical double layer at the
67 mineral-brine interface (Figure *1* (a)); decreasing the total ionic strength increases the magnitude
68 of the zeta potential in a process often termed 'double layer expansion' [10].
69
70 In contrast to oxides of metal or semi-metals, such as quartz [10], pH does not directly control the
71 zeta potential of carbonate mineral surfaces; rather, varying the pH controls the equilibrium
72 concentration of $Ca^{2+}$and Mg^{2+} for a given CO_2 partial pressure (pCO_2), and it is the concentration
73 of Ca^{2+} and/or Mg^{2+} that controls the zeta potential [11-13]. Despite this, many studies still report
74 measurements of zeta potential on carbonates as a function of pH [3, 7, 8, 11, 14-19]. The apparent

correlation between pH and zeta potential obtained in these studies reflects the relationship between pCa (calcium concentration, expressed as the negative decimal logarithm of the calcium concentration in M) and zeta potential, with pCa varying in response to the imposed variation in pH. It is not possible to retrospectively extract the relationship between zeta potential and pCa from these studies, because calcium concentration was typically not measured. A relationship between SO_4^{2-} concentration and carbonate zeta potential has also been proposed, with increasing SO_4^{2-} yielding more negative zeta potential [2-4, 7, 8, 11, 14-17, 20, 21]; alternatively, it has been suggested that SO_4^{2-} only indirectly affects zeta potential by modifying the equilibrium concentration of Ca^{2+} [11, 12]

Previous studies have shown that the experimental conditions during zeta potential measurements are particularly important in carbonates to ensure consistent and repeatable data: it is essential to ensure that equilibrium has been reached between the mineral surfaces and the brine of interest, which may require 10's or even 100's hours of pre-equilibration to achieve [12]; it is also important to control (or measure) pCO_2, as different pCO_2 (e.g. in open versus closed system experiments) will yield different equilibrium concentrations of Ca^{2+} [12, 17]. Some of the observed variability in zeta potential data in natural carbonates may reflect failure to reach equilibrium, or unknown/unreported variations in pCO_2.

Despite the large number of published measurements of zeta potential in carbonates [12], few measured data are relevant to carbonate oil reservoirs. Most studies obtain zeta potential data using commercially available laboratory equipment (such as a zetasizer) that measure electrophoretic mobility [e.g. 4, 16, 19, 22-26]. These devices have a limited range of operating conditions that are far from those present in natural oil reservoirs. Rock samples must be crushed to a sub-grain size powder, destroying the natural textures and exposing fresh mineral surfaces to the brine that would not be present in nature. Moreover, measurements in the high concentration

electrolytes (>0.5M) and elevated temperatures (>60ºC) typical of oil reservoirs are difficult to perform, because (i) it is challenging to maintain a stable suspension of the powder in the brine of interest, (ii) pressurized sample containers are required to avoid evaporation and electrolyte loss, and (iii) the electrodes degrade rapidly. Finally, only one fluid phase is present in a given experiment, unlike the mixed wettability and multiphase fluids present in natural oil reservoirs. The streaming potential method, first described by [43], is less commonly used but can overcome some of the limitations of conventional measurements of electrophoretic mobility, as it can be used to measure the zeta potential of intact rock cores at elevated temperature, saturated with multiple fluids including brines of high ionic strength [28,29].

The relatively limited relevant data published to date suggest that the zeta potential on natural, intact calcium carbonates in equilibrium with natural formation brines is typically positive, owing to the high concentration of Ca^{2+} in such brines, but is negative in lower salinity brines such as seawater, reflecting the lower Ca^{2+} concentration and, possibly, higher SO_4^{2-} concentration [11, 12, 20]. However, different natural samples can exhibit different zeta potential values in the same brine, which may reflect differences in the texture, structure and mineral distribution across samples, or trace impurities and organic material on the mineral surfaces [11]. The impact of these small-scale variations on zeta potential may be lost in studies where samples are crushed in order to be measured [4, 16, 19]. Moreover, most data published to date were obtained at laboratory conditions.

Al-Mahrouqi et al. [27] measured the temperature dependence of the zeta potential in intact natural carbonates and found that the zeta potential became smaller in magnitude with increasing temperature in low concentration brines (0.01M) but was independent of temperature in high concentration brines (>0.5M). However, they explored simple NaCl brines in which the Ca^{2+} present was sourced only from dissolution of the sample during initial equilibration; the

127 temperature dependence of zeta potential in these experiments was directly correlated with the
128 temperature dependence of the measured equilibrium Ca^{2+} concentration. As yet, measurements
129 of the zeta potential in natural carbonates saturated with oilfield brines of interest at elevated
130 temperature are scarce, which motivates the first aim of this paper: to expand the experimental
131 dataset by reporting measurements of zeta potential obtained in five intact reservoir carbonate
132 samples and two outcrop carbonate samples, saturated with three synthetic formation brines,
133 synthetic seawater, and three synthetic low salinity brines representative of those used in CSW.
134 Data are obtained at laboratory temperature, and also elevated temperature relevant to oil reservoir
135 conditions.
136
137 Previous studies have shown that the zeta potential in natural carbonates saturated with brine and
138 crude oil is affected by the wetting state i.e. whether brine or oil preferentially wets the mineral
139 surfaces. Jackson and Vinogradov [28] measured a positive zeta potential on natural, water-wet
140 reservoir carbonates which became less positive after aging in crude oil. They proposed that the
141 zeta potential at oil-wet mineral surfaces reflects the oil-brine interface rather than the mineral-
142 brine interface (Figure 1 (b)); in their model, a more negative zeta potential measured in an oil-wet
143 sample is consistent with a negative zeta potential at the oil-brine interface. Jackson et al. [9]
144 extended this work and reported a correlation between wettability and the change in zeta potential
145 after aging. However, of the four crude oils tested in their work, they found only three yielded
146 increasingly negative zeta potential after aging, consistent with a negative oil-brine zeta potential.
147 One crude oil yielded increasingly positive zeta potential, consistent with a positive oil-brine zeta
148 potential. This result was unexpected: although measurements of the zeta potential at the oil-brine
149 interface are scarce, they usually return negative zeta potential at pH values relevant to carbonate
150 oil reservoirs and the experiments undertaken by [9] [e.g. [23, 24]]. Consequently, there is a risk
151 that the single crude oil in the study of [9] that returned an apparently positive oil-brine zeta
152 potential is an outlier, not typical of crude oils in general. Moreover, [9] used only a single

153 carbonate rock type. These observations motivate the second aim of this paper: to expand the
154 experimental dataset by reporting measurements of zeta potential after aging the five intact
155 reservoir carbonate samples and two outcrop carbonate samples introduced above in three new
156 crude oils.
157
158 Jackson et al. [9] correlated, for the first time, changes in zeta potential observed in response to
159 changing brine composition, and changes in zeta potential observed after aging, to IOR during
160 CSW. They proposed a model for CSW in which IOR is observed only if the chosen injection
161 brine yields a change in zeta potential at the mineral-brine interface that causes an increase in the
162 electrostatic repulsion between the mineral-brine and oil-brine interfaces. Thus, the mineral
163 surface zeta potential should be made more negative to yield IOR for crude oils with a negative
164 oil-brine zeta potential, but made more positive to yield IOR for crude oils with a positive oil-
165 brine zeta potential. They tested the model in coreflooding experiments and found that simple
166 dilution, from formation brine to dilute seawater (i.e. a conventional low salinity waterflood, LSW)
167 yielded more negative mineral surfaces and successful IOR for the three crude oils interpreted to
168 have a negative oil-brine zeta potential. However, the conventional LSW did not yield IOR for
169 the crude oil interpreted to have positive oil-brine zeta potential. Only an inverse LSW (i.e.
170 switching from low salinity brine to formation brine), producing more positively charged mineral
171 surfaces, yielded successful IOR for the oil interpreted to have a positive oil-brine zeta potential.
172 The inverse LSW did not yield IOR for the crude oils interpreted to have a negative oil-brine zeta
173 potential. Thus, the CSW model of Jackson et al. [9] was able to successfully predict when a
174 conventional LSW would yield IOR; it was also, uniquely, able to predict when a non-conventional
175 inverse LSW would yield IOR. Jackson et al. [9] suggested that LSW failures reported in previous
176 studies were because the crude oil of interest had a positive oil-brine zeta potential that had not
177 been recognized.
178

179 The model of CSW developed by Jackson et al. [9] has been tested so far only on one carbonate
180 rock specimen and four crude oils. The third aim of this paper is therefore to test Jackson's CSW
181 model using the five intact reservoir carbonate samples, two outcrop carbonate samples and three
182 new crude oils introduced above. Overall, the paper reports a new suite of integrated experimental
183 measurements of zeta potential and oil recovery during CSW in carbonates that further test the
184 Jackson model of CSW.
185

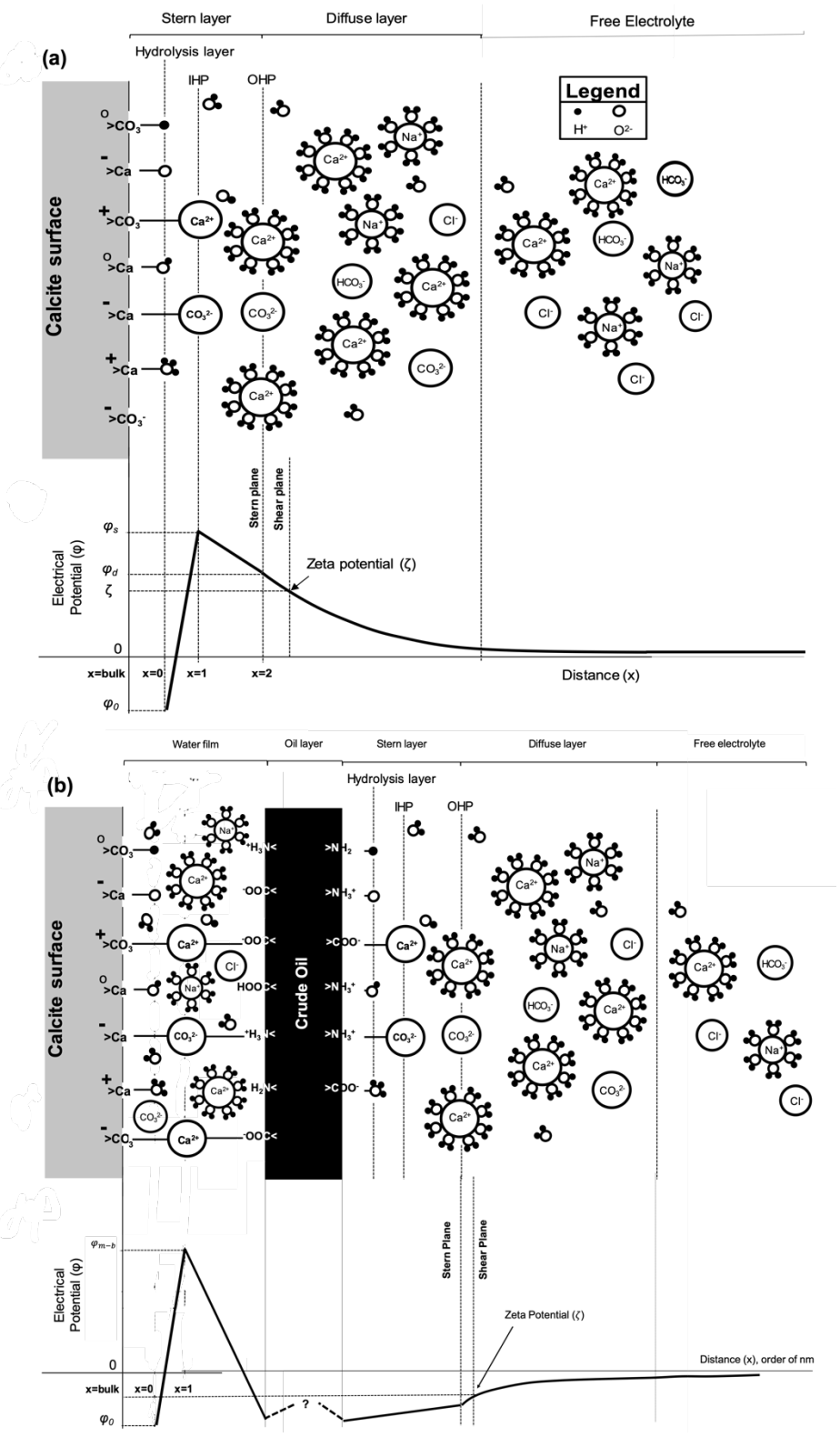

186

187

188 **Figure 1** - Schematic of a triple layer model for (a) the mineral-brine interface [11] and (b) the same interface after

189 aging and wettability alteration with a negatively charged crude oil. The crude oil is attached to the mineral surface via

ion bridges (e.g. Ca^{2+}, CO_3^{2-}) within a thin water film between the two interfaces. On a water-wet surface (a), the zeta potential is dictated by the properties of the mineral-brine interface; however, on an oil-wet surface, the zeta potential is dictated by the properties of the oil-brine interface.

Materials and Methods

Materials

Table 1 summarises the materials used in this study. Samples of outcrop carbonates were used along with a range of reservoir samples for which we cannot disclose mineralogical data due to commercial sensitivity. The crude oil samples labelled SR-A to SR-D were previously studied by Jackson et al., [9] and all measurements using these crude samples were made on samples of Estaillades natural carbonate rock. Artificial brines were prepared using deionised water and reagent grade salts.

Table 1 - Materials used in this study. Oils SR-A to SR-D were previously reported by Jackson et al., [9].

Carbonate Core Samples									
Sample	**BA**	**BB**	**BC**	**BD**	**BF**	**BG**	**BH**	**TE**	**TR**
Description	Reservoir	Reservoir	Reservoir	Reservoir	Reservoir	Reservoir	Reservoir	Outcrop	Outcrop
Permeability (mD)	10 +/- 2	10 +/- 2	120 +/- 20	10 +/- 2	25 +/- 5	10 +/- 2	10 +/- 2	85 +/- 10	20 +/- 5
Formation Factor (F)	35	20	25	20	50	35	20	40	20
Mineralogy	N/A	N/A	N/A	N/A	N/A	N/A	N/A	>99% Calcite	>99% Calcite

Brine Compositions (salt concentrations in ppm)							
Brine Type	**Formation Brine**			**Seawater**	**Low Salinity Brine**		
Brine Name	**BFB1**	**TFB1**	**BFB2**	**TSW**	**BLS1**	**TLS1**	**BLS2**
NaHCO3	0	200	0	156	0	1	220
NaCl	89,442	109,550	177,440	29,000	648	760	90
CaCl2.2H2O	12,800	46,070	40,440	605	46	20	616
MgCl2.6H2O	12,827	11,240	21,040	405	186	296	903
KCl	0	0	2,190	900	0	35	13
SrCl2.6H2O	0	0	1,900	0	0	0	9
Na2SO4	0	140	1,020	26	0	87	1,000
NaBr	0	0	690	0	0	0	0
LiCl	0	0	30	0	0	0	0

TDS (ppm)	115,069	167,200	244,750	31,092	881	1,199	2,852
IS (mol/L)	1.99	3.03	4.29	0.53	0.01	0.02	0.05

Oil Properties

Oil Name	Acid Number (mg/KOH)	Base Number (mg/KOH)
SR-A [9]	0.15	0.80
SR-B [9]	0.20	1.77
SR-C [9]	0.05	0.40
SR-D [9]	0.20	1.20
Oil BD	0.05	0.60
Oil BM	0.20	1.80
Oil TT	0.34	0.41

Zeta Potential Measurements

The streaming potential apparatus of Vinogradov et al. [29] was used to obtain the zeta potential measurements. Only a brief summary of the method is provided here; for additional details, see [9, 29]. Figure 2 shows a schematic of the experimental apparatus, which uses a non-metallic core holder, adapted to include two Ag/AgCl electrodes situated on either side of the core holder and out of the direct path of the flow, to measure the voltage difference across the core. A pump is used to induce brine flow through the core, using a light mineral oil as a hydraulic fluid to force the brine out of the inlet reservoir and through the sample to the outlet reservoir, creating a pressure drop across the sample. The direction of brine flow through the core can be reversed. The setup ensures the brines are isolated from air within a closed system which maintains a constant atmospheric pCO_2 [17]. The core holder and reservoirs can be placed inside an oven to measure zeta potential at elevated temperatures up to 150°C [27, 30]. Experiments here were conducted at laboratory temperature, or at elevated temperatures of 70°C, 80°C or 100°C. Prior to each experiment the rock samples were equilibrated with the brine of interest for at least 24 hours.

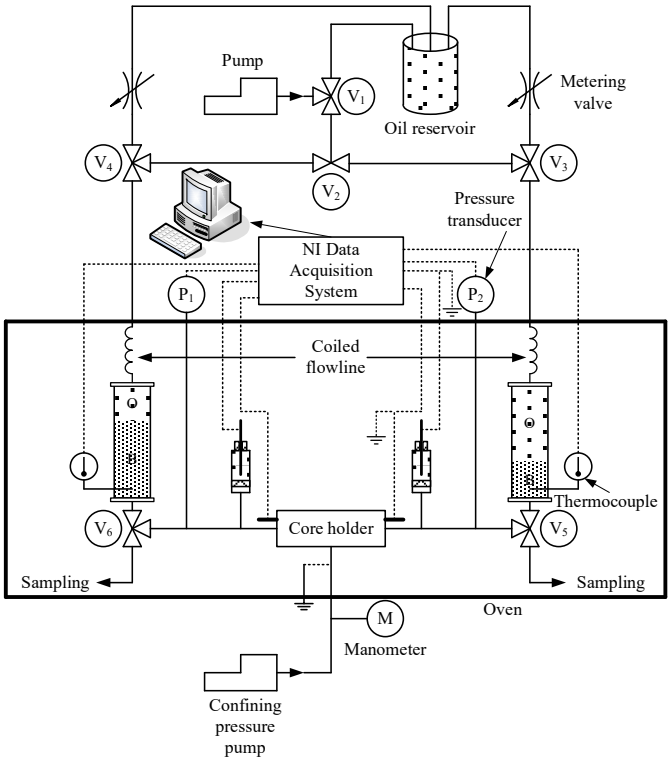

Figure 2 - Schematic of the experimental apparatus used to measure the zeta potential, modified from [29].

Stabilised pressure and voltage measurements were recorded for a number of different flow rates, typically five to eight per zeta potential measurement, with flow reversed at each flow rate to ensure the pressure and voltage responses are symmetric with respect to flow direction. Plotting the stabilised voltage difference against the stabilised pressure difference for each flow rate allows determination of the streaming potential coupling coefficient (C), given by the gradient of a linear regression through the data. The zeta potential can then be calculated using a form of the Helmholtz-Smoluchowski equation given by [31]:

$$C = \frac{\partial V}{\partial P} = \frac{\varepsilon_w \zeta}{\mu_w \sigma_{rw} F} \qquad (1)$$

The intrinsic formation factor ($F = \sigma_{bb}/\sigma_{rwb}$) represents the ratio of brine electrical conductivity (σ_{wb}) to saturated rock electrical conductivity (σ_{rwb}), measured using high ionic strength electrolyte

(denoted by the subscript *h*) to ensure the contribution of surface electrical conductivity is negligible.

Equation (1) is derived assuming that (i) the diffuse layer thickness is much less than the pore-size (the so called "thin double layer approximation"; see [45]) and (ii) that the variation in excess charge through the diffuse layer can be assumed linear (see [10]). Both these assumptions are valid in high ionic strength brines. The form of equation (1) used here accounts for the contribution of surface electrical conductivity in low ionic strength brines [31]. Thus, there is no restriction on application of equation (1) to calculate zeta potential for the brine compositions used in this study. Following the approach of Vinogradov et al. [29], the brine conductivity (σ_w) and the saturated rock conductivity for the brine of interest (σ_{rw}) were measured in each experiment, while the brine viscosity (μ_w) and permittivity (ε_w) were calculated using published correlations [32].

Coreflooding Experiments

The coreflooding experimental workflow broadly followed that of Jackson et al. [9]. Initially, mineral-brine zeta potential measurements were made using the methodology described above. Data were obtained at the temperature of interest for each of the brines of interest (Table 1). The coreflooding procedure for a given sample began with the sample saturated in the aging brine of interest. The sample was then drained with the crude oil of interest at a low rate until the irreducible water saturation had been reached; the chosen rate depended on rock permeability but was typically in the range 0.01 – 0.5mL/min (1.5×10^{-7} – 7.4×10^{-6} m/s). A minimum of 10 pore volumes (PV) of the crude oil were drained through the core. The core was then statically aged in an Amott cell at 80°C for a minimum of four weeks, immersed in the aging crude oil. Following aging, the oil in the Amott cell was replaced with the aging brine and a spontaneous imbibition test was performed for a further three weeks at the chosen coreflooding temperature.

The volume of water spontaneously imbibed was recorded and the sample then waterflooded with the aging brine until the first residual oil saturation (S_{or}) was reached, identified when coreflooding of at least 2PV yielded no additional oil. The volume of oil recovered was recorded as a function of PV injected, along with the flowrate of brine and the pressure drop across the core. At S_{or}, when there was only brine flowing through the core, the streaming potential was measured again using the same methodology as described previously. Wettability change was characterised by the Amott water wetting index given by:

$$I_w = \frac{V_{SI}}{V_{SI} + V_{FI}} \quad (2)$$

where V_{SI} is the volume of water spontaneously imbibed and V_{FI} is the additional volume of water that can be forced into the sample.

The injection brine was switched to the controlled salinity brine of interest and any additional oil recovered by the CSW brine measured. The streaming potential was also measured at each subsequent value of S_{or}.

For repeat experiments, samples were cleaned in a Soxhlet unit using toluene and methanol heated under reflux for several days, with regular replacement of the solvents until there was no further colour change of the solvents in the lower flask. Samples were dried for 24hrs to remove residual solvents. Petrophysical properties were then measured again to confirm cores had returned to their original state.

To ensure consistency across corefloods, the flowrate was chosen to ensure the capillary number was similar in magnitude. The capillary number used is defined as:

$$Ca = \frac{\gamma . A}{\mu_w L Q} \sqrt{\emptyset . k} \quad (3)$$

Where γ is the interfacial tension of the oil-brine, assumed to be 35mN/m for all crude oils. The remaining properties were all measured or calculated as part of our standard workflow. L is the sample length, A is the sample cross sectional area, ϕ the sample porosity, k the single-phase permeability and Q the volumetric flow rate through the core, which was varied across experiments to keep the capillary number consistent. Capillary numbers used in corefloods were initially of the order 18-20 (all properties defined in SI units) with high flowrate 'bumps' at capillary numbers of approximately 12, 6 and 2 conducted when the residual saturation had been reached, to ensure any increases in oil recovery observed upon CSW brine injection were not the result of capillary end effects.

Results

Carbonate-Brine Zeta Potential

We begin by reporting the zeta potential in samples saturated with reservoir relevant brines at both laboratory and elevated temperature. The zeta potential of the carbonate-brine interface is necessary to understand how modifying the injection brine composition changes the electrostatic forces acting at COBR interfaces during CSW. Figure 3 shows zeta potential measured at ambient conditions on the intact outcrop and reservoir carbonate samples investigated here, saturated with complex brines typical of those used in CSW (Table 1). The equilibrium pH of the effluent brine is also reported for each measurement.

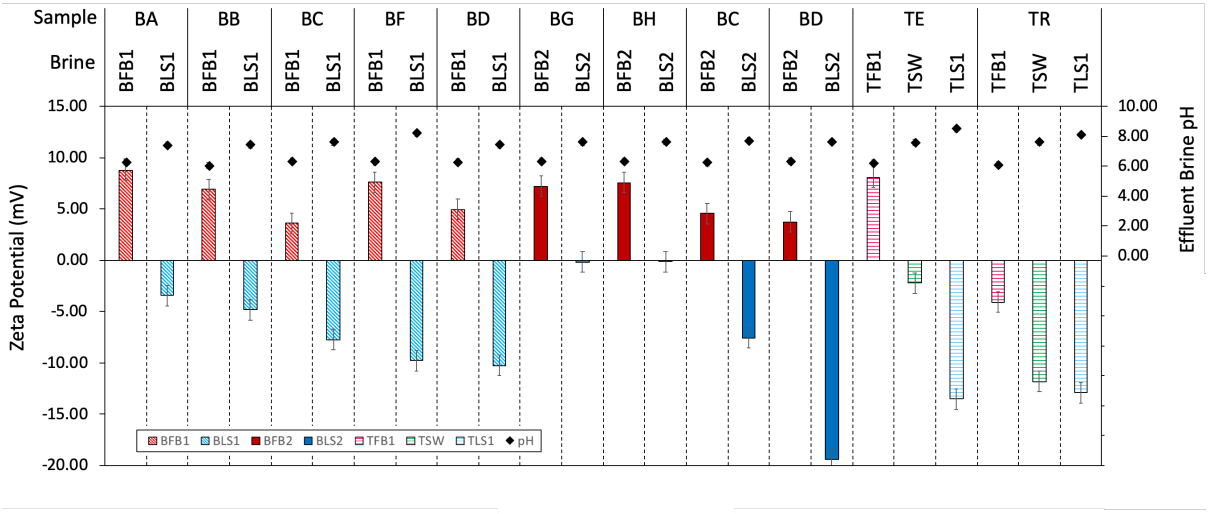

Figure 3 - Mineral-brine zeta potential measurements at ambient conditions for the carbonate samples and brines reported in Table 1. Bars represent zeta potential with the different shades and colours corresponding to different brines; diamonds show equilibrium effluent brine pH. The results of repeat experiments on selected samples (BC, BD, BH, TR and TE) can be found in the supplementary materials.

Generally, the zeta potential in formation brines was positively charged and small in magnitude (< 10 mV), consistent with previous published data [e.g. 11] and reflecting the high concentrations of Ca^{2+} and Mg^{2+} (Table 1). However, a notable exception was sample TR. This was the only

carbonate sample reported to date which has returned a negative zeta potential in formation brine. Seawater saturated samples yielded negative zeta potential values that are again small in magnitude (<5 mV) and again consistent with those reported previously [e.g. 11]. In the low salinity brines, the zeta potential was always negative, but with a large variation in magnitude across the different samples, with sample BD returning -19 mV but samples BG and BH only –1 mV. Note that the change in streaming potential during the experiments on BG and BH was clearly in the opposite sense to the change in pressure [see 12 for examples of raw streaming potential and pressure data] so we are confident the zeta potential was negative, despite the small magnitude.

Variations in the magnitudes for different samples or different brines would be expected based on previous published data [11, 12]. However, samples BC and BD are from the same subsurface reservoir formation yet returned zeta potential that differed significantly in magnitude, especially in low salinity brines; moreover, samples TR and TE are compositionally indistinguishable, but returned not only differences in the magnitude of the zeta potential, but also opposing polarity when saturated with the same brine. Repeat measurements on these same samples with the same brines confirmed the data reported here.

There is no observed correlation between the variable zeta potentials observed across the samples and other parameters that are known control zeta potential in carbonates. The equilibrium brine pH was typically in the range 5-8, increasing with decreasing brine salinity and correlating with pCa, consistent with the trend reported by [11]. However, no correlation between zeta potential and pCa and/or pH was observed that could explain the variability between samples for the same brines. Measurements of pCa in the effluent brine showed no significant differences from the values given in Table 1, so did not measurably change during equilibration. We suggest the variable zeta potentials reflect differences in the texture, structure and mineral distribution across samples, or trace impurities and organic material on the mineral surfaces [11].

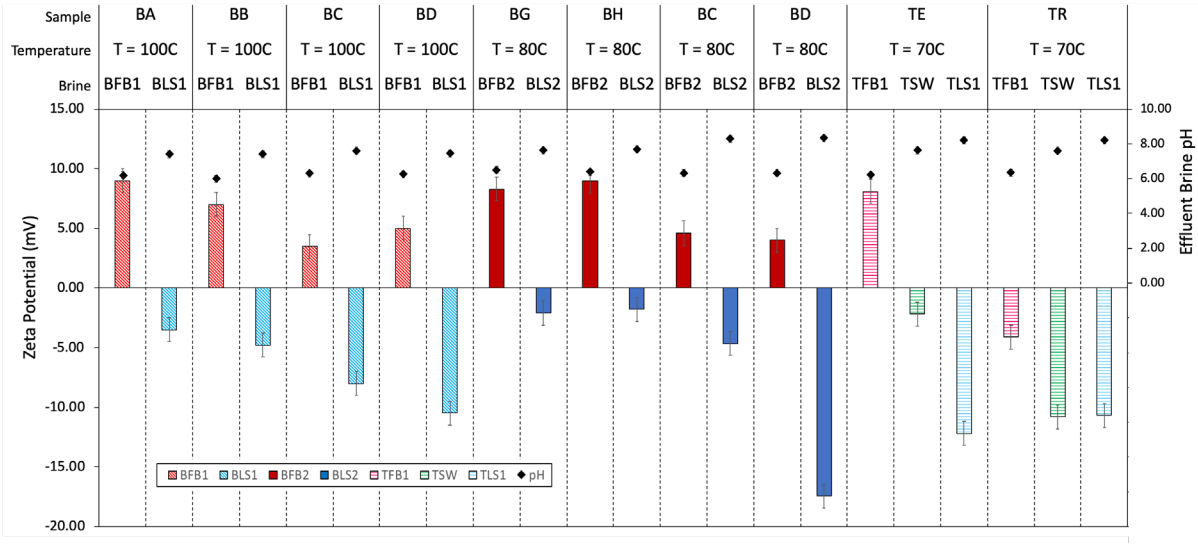

Figure 4 - Mineral-brine zeta potential measurements at elevated temperature conditions for the carbonate samples and brines shown in Figure 3 and reported in Table 1. Bars represent zeta potential with the different shades and colours corresponding to different brines; diamonds show equilibrium effluent brine pH. Additional single phase measurements made during repeated experiments on certain samples (BC, BD, BH, TR and TE) can be found in the supplementary materials.

The main trends observed at laboratory temperature were replicated at elevated temperature (Figure 4). Zeta potential measurements were positive in formation brine, with the exception of sample TR which again returned negative zeta potential. The zeta potential for all samples was negative in seawater and the dilute brines. The pH again correlated with pCa, and no consistent or significant changes in equilibrium pH were observed between ambient and elevated temperature.

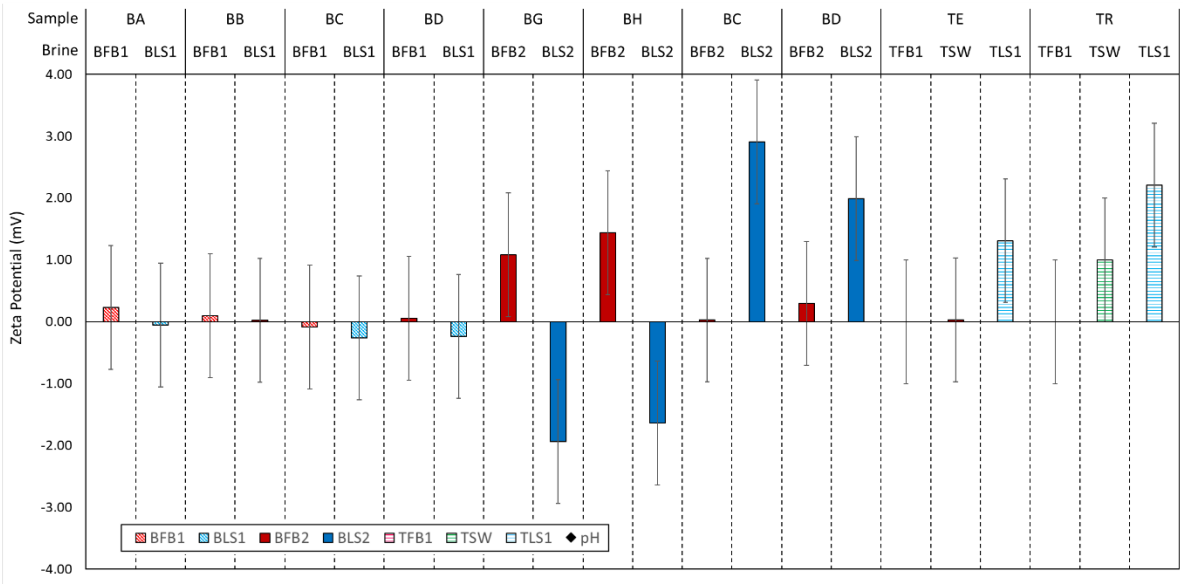

Figure 5 – Change in zeta potential from ambient to elevated temperature for the carbonate samples and brines shown in Figures 3 and 4, and reported in Table 1.

Overall, our data suggest that temperature does not play a consistent or significant role in modifying zeta potential for carbonates saturated with complex, mixed brines. Of the samples and brines tested here, the zeta potential was identical within experimental error at low and high temperature for 14 of the 22 carbonate/brine combinations tested (Figure 5). In the remaining 8 carbonate/brine combinations, the zeta potential became more positive in formation brine at high temperature for two carbonate samples, and more negative at high temperature in dilute brine for the same two samples. However, the zeta potential became more positive in seawater and dilute brine in the other samples. No change in pH outside of experimental error was observed between ambient and elevated temperature. Thus, the change in zeta potential caused by changing the brine composition (which we term here $\Delta\zeta_{CSW}$) was essentially independent of temperature (Figure 6). Injection of a dilute brine, as in a conventional low salinity waterflood, yields a more negative zeta potential at the mineral-brine interface irrespective of temperature and carbonate sample tested. However, the magnitude of the change in zeta potential depends on carbonate sample, with the smallest change observed of -8 mV for sample BG and BH at laboratory temperature, and the largest of -24 mV observed for sample BD, also at laboratory temperature (Figure 6).

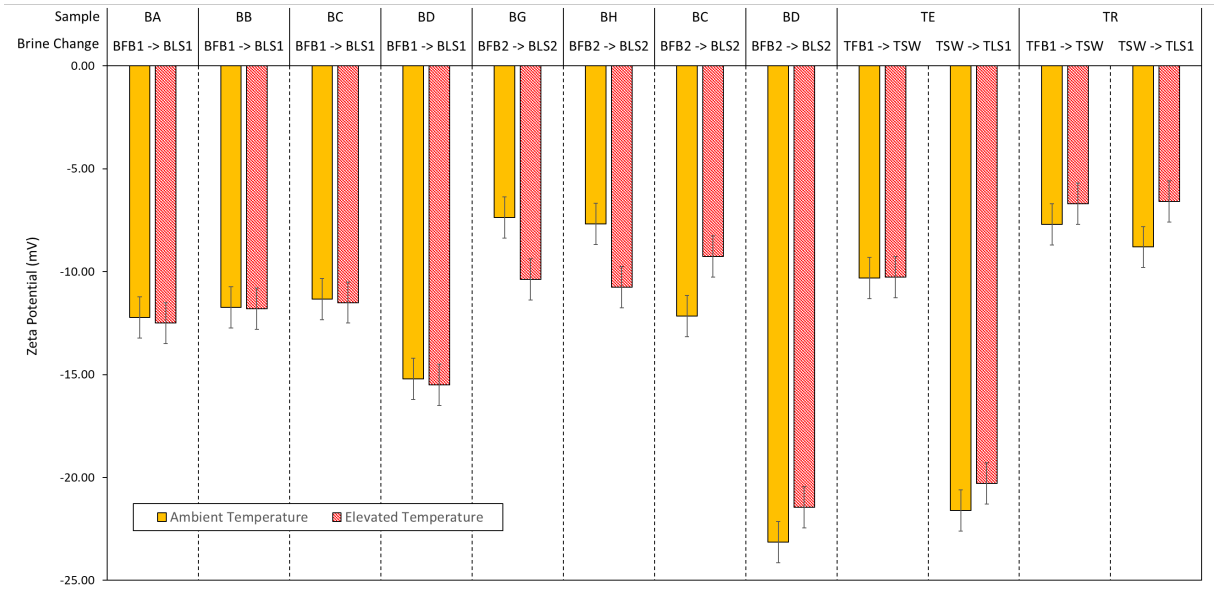

Figure 6 – Change in zeta potential between high and low ionic strength brines at both ambient and elevated temperature for various carbonate samples and brine compositions.

Zeta Potential and Wettability

Figure 7 shows the effect of wettability alteration on the zeta potential for several different samples and crude oils initially saturated with formation brine. The zeta potential of the fully water saturated samples (S_w=1) and the same samples at residual oil saturation ($S_w = 1 - S_{or}$) after aging are shown, along with the difference between these two values (which we term here $\measuredangle\zeta_{wett,}$) which represents the change in zeta potential caused by wettability alteration.

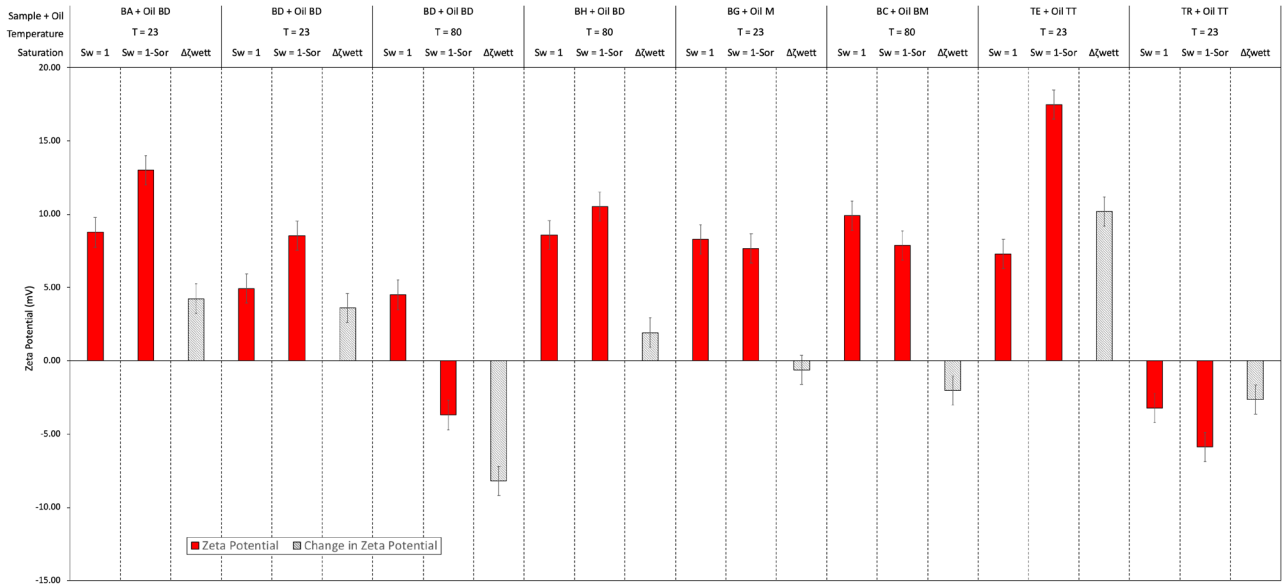

Figure 7 - Zeta potential measurements made at $S_w = 1$ and $S_w = 1 - S_{or}$ in samples aged when saturated with formation brine and crude oil, along with the difference between these values ($\Delta\zeta_{wett}$). The temperature here reflects the temperature at which the zeta potential was measured. Aging of the samples was always undertaken at elevated temperature (see Method).

In this work, three crude oils were used. Aging in Oil BM and formation brine consistently caused the zeta potential to become more negative, irrespective of the carbonate sample used or the experimental conditions. Aging in Oil TT and formation brine caused the zeta potential to become more positive in sample TE, but more negative in sample TR. This is the only combination of crude oil and carbonate sample in which the change in zeta potential after aging is sample specific across all of the crude oils and carbonate samples tested here and by [9]. The change in zeta potential of samples aged in Oil BM was measured at ambient and elevated temperature and was always of the same polarity. In contrast, aging in Oil BD and formation brine caused the zeta potential to become more positive at laboratory temperature, but more negative at elevated temperature (Figure 7). The magnitude of the change in zeta potential varied across samples, crude oils and experimental conditions as with the single-phase mineral-brine zeta potential measurements. Oil BM typically caused a smaller change in the zeta potential after aging of approximately -1mV whereas Oil BD caused a much larger change of up to +5mV. Oil TT showed

a very large change in sample TE of +10mV but a smaller change in sample TR of -3mV. Effluent brine pH values recorded during the streaming potential measurements at S_{or} were comparable to those recorded at full water saturation.

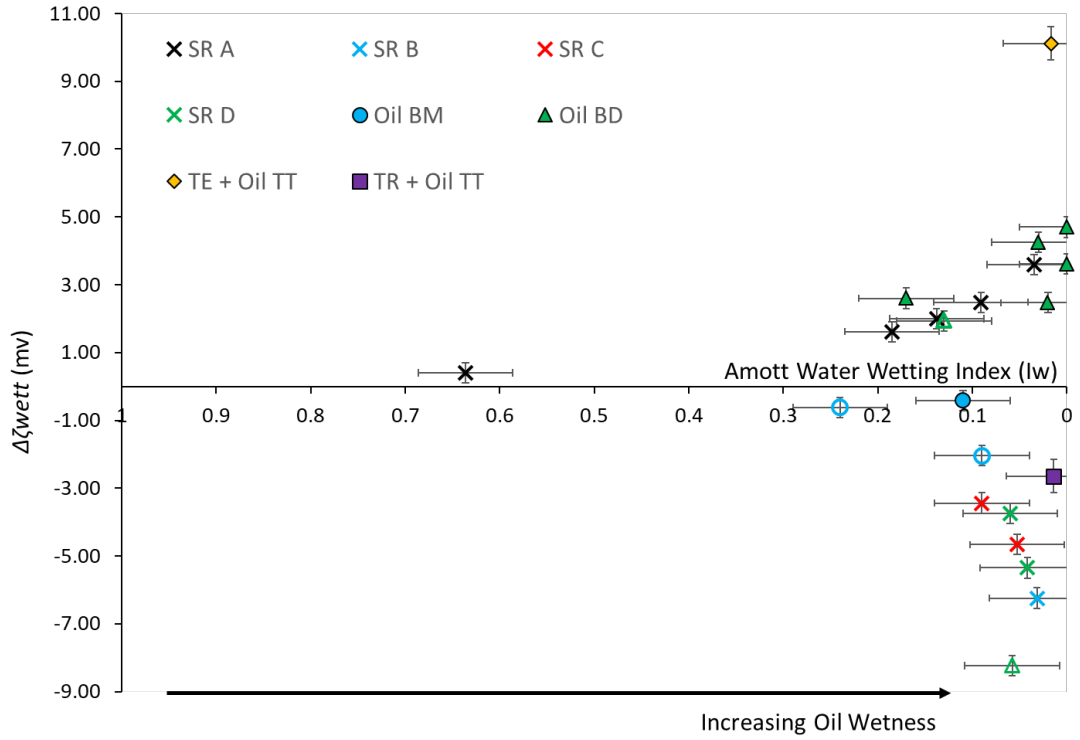

Figure 8 - Change in zeta potential measured in formation brine after aging for a range of crude oils, carbonate samples, formation brine compositions and temperatures. Filled symbols represent data obtained at ambient temperature. Open symbols represent data obtained at elevated temperature. Data for oils SR-A to SR-D previously reported [9] and shown by crosses. TE+Oil TT denotes the results of aging sample TE in crude oil TT; TR+Oil TT denotes the results of aging sample TR in crude oil TT. All other crude oils showed similar behaviour irrespective of rock sample, so the rock sample is not reported.

A plot of $\Delta\zeta_{wett}$ against the Amott water wetting index (I_w) for each crude oil and shows two main trends (Figure 8). Smaller values of I_w correspond to more oil-wet cores. An I_w value of 1 corresponds to the fully water saturated state. Filled data points represent measurements made at ambient temperature and open data points represent measurements made at elevated temperature. For ambient temperature results, two crude oils (SR-A, BD) show an increasingly positive zeta potential with decreasing I_w and increasing oil wetness. Four crude oils (SR-B, SR-C, SR-D and

417 BM) show an increasingly negative zeta potential with decreasing I_w and increasing oil wetness.
418 Oil TT deviates from these trends, showing both a positive and negative change in zeta potential
419 after aging in formation brine that is dependent on carbonate sample type. Oil BD also exhibits
420 both positive and negative changes dependent on the temperature, as noted previously.
421
422 Jackson and Vinogradov [28] and Jackson et al. [9] interpreted the change in zeta potential after
423 aging in terms of the zeta potential at the oil-brine interface. They argued that a positive change
424 in $\Delta\zeta_{wett}$ is consistent with a positive zeta potential at the oil-brine interface and vice-versa because,
425 after aging and wettability alteration, the oil-wet mineral surfaces return the zeta potential of the
426 oil-brine interface rather than the mineral brine interface (Figure 1). Jackson [44] demonstrated
427 that the zeta potential interpreted from the streaming potential across a bundle of capillary tubes
428 model tends towards the value of the oil-brine interface as the tubes become increasingly oil-wet.
429 The exact nature of the relationship between wettability and zeta potential in rocks will depend in
430 a complex way on the pore-scale distribution of wettability and flow.
431
432 It is important to note that the polarity of the oil-brine zeta potential interpreted in this way can
433 be ambiguous. If the zeta potential is initially positive and becomes more positive after aging, then
434 this unambiguously indicates a positive oil-brine zeta potential (e.g. oil BD and samples BA, BD
435 and BH at laboratory temperature in Figure 7). Likewise, if the zeta potential is initially negative
436 and becomes more negative after aging, then this unambiguously indicates a negative oil-brine zeta
437 potential (e.g. oil TT and sample TR in Figure 7). If the zeta potential is initially positive and
438 becomes negative after aging, then this unambiguously indicates a negative oil-brine zeta potential
439 and vice-versa (e.g. oil BD and sample BH at elevated temperature in Figure 7). However, if the
440 zeta potential is initially positive and becomes less positive after aging, then this could indicate a
441 negative or less positive zeta potential at the oil-brine interface (e.g. oil BM in Figure 7); likewise,
442 if the zeta potential is initially negative and becomes less negative after aging, then this could

443 indicate a positive or less negative zeta potential at the oil-brine interface. We acknowledge this
444 ambiguity when recording the interpreted zeta potential for each crude oil (e.g. Table 2).
445
446 In addition to aging in formation brine, Jackson et al., [9] also investigated the effect of wettability
447 alteration on the zeta potential when aging in low salinity brine with two crude oils (SR-A and SR-
448 D). They found that the change in the zeta potential after aging in low salinity brine was of the
449 same polarity (but different magnitude) as when aged in formation brine, and thus concluded that
450 the polarity of the zeta potential of the oil-brine interface was independent of brine composition
451 or ionic strength at pH values relevant to carbonate oil reservoirs. We further tested this
452 hypothesis here with several rock samples and crude oils. The zeta potential of these samples
453 measured at $S_w = 1$ and $S_w = 1 - S_{or}$ along with the change in zeta potential after aging these samples
454 in low salinity brine ($\Delta\zeta_{wett}$) is shown in Figure 9.
455

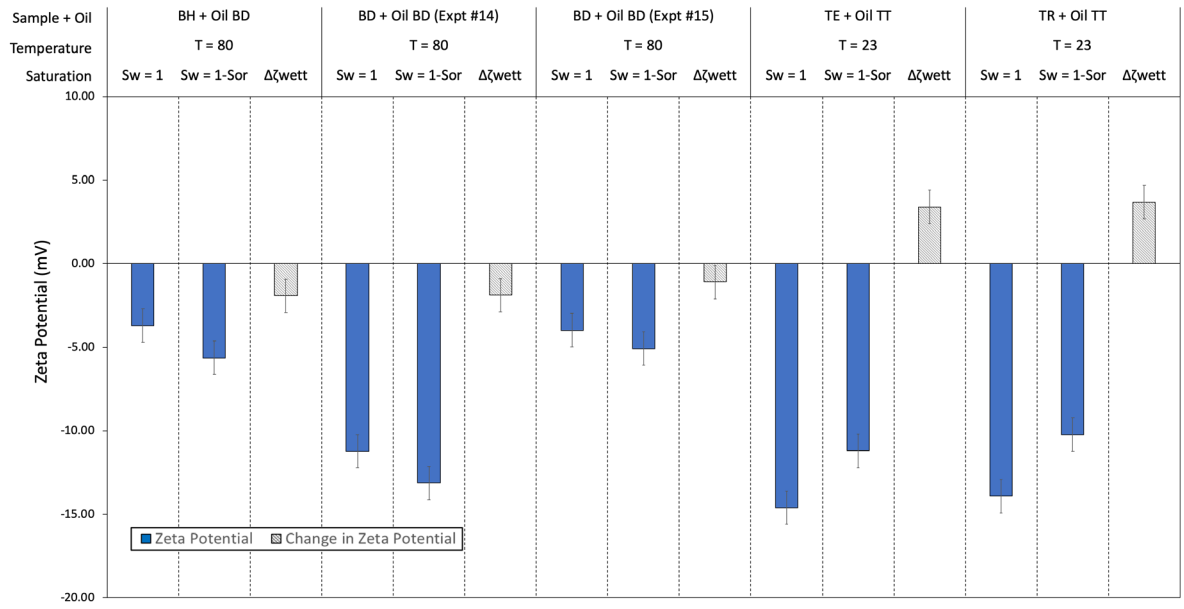

456

457 **Figure 9** - Zeta potential measurements made at $S_w = 1$ and $S_w = 1 - S_{or}$ in samples aged when saturated with low
458 salinity brine and crude oil, along with the difference between these values ($\Delta\zeta_{wett}$). The temperature here reflects the
459 temperature at which the zeta potential was measured. Aging of the samples was always undertaken at elevated
460 temperature (see Method).

As with the measurements made after aging in formation brine, there is a potential ambiguity in the interpretation of the oil-brine interface polarity. In low salinity brine, the zeta potential of the mineral-brine interface is always negative. Those samples which show a more negative zeta potential after aging and wettability alteration (Samples aged with Oil BD in Figure 9 unambiguously indicates a negative oil-brine zeta potential, however, in those samples where the zeta potential became less negative after aging (Samples aged with Oil TT in Figure 9) could represent either a positive or less negative oil-brine zeta potential. The change in zeta potential for samples saturated and aged in low salinity brine ($\Delta\zeta_{wett}$) as a function of I_w is plotted in Figure 10. Again, filled symbols represent measurements made at ambient temperature while open symbols represent those made at elevated temperature.

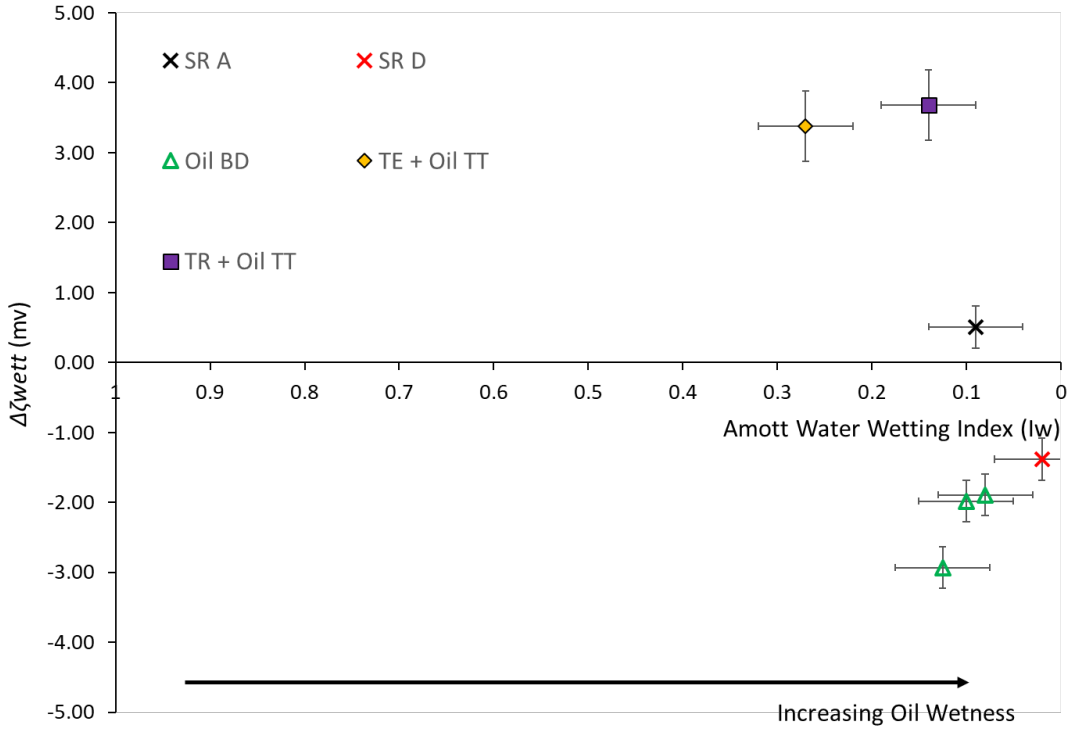

Figure 10 - Change in zeta potential measured in low salinity brine after aging for a range of crude oils, carbonate core samples, low salinity brine compositions and temperatures. Filled symbols represent data obtained at ambient temperature. Open symbols represent data obtained at elevated temperature. Data for oils SR-A to SR-D previously reported by [9] and shown by crosses. TE+Oil TT denotes the results of aging sample TE in crude oil TT; TR+Oil TT denotes the results of aging sample TR in crude oil TT.

We find here that the polarity of $\Delta\zeta_{wett}$ for a given crude oil is different depending on whether the aging was in formation or low salinity brine (Figure 10; compare like crude oils with Figure 8). After aging in formation brine, oil BD generally caused the zeta potential to become more positive; however, when aging in low salinity brine, the opposite trend was observed. Oil TT, which was observed to show both a positive and negative change in zeta potential after aging in formation brine dependent on the core sample type, consistently caused the zeta potential to become more positive irrespective of core type after aging in low salinity brine and the change was of comparable magnitude (+3.5mV).

The data presented here and by Jackson et al., [9] report results showing the link between wettability alteration and changes in the zeta potential for seven different crude oils. When aging in formation brine, four of these oils (SR-B, SR-C, SR-D and BM) have consistently caused the zeta potential to become more negative in all samples; one (SR-A) consistently resulted in a more positive zeta potential, and two have shown both a more positive and more negative zeta potential depending on the rock sample or temperature (BD and TT). Samples aged with either Oil TT or Oil BD exhibit more positive or more negative zeta potentials depending on the core type, aging brine and conditions used. Assuming that the change in zeta potential after aging is indicative of the zeta potential of the oil-brine interface, then the data reported here suggest that the zeta potential of the oil-brine interface depends not only on the crude oil properties (as suggested by [9]) but also on the host rock, brine salinity and/or composition, and temperature. Controls on the zeta potential at the oil-brine interface and the implications for CSW will be discussed later.

Controlled Salinity Corefloods

Two types of corefloods were performed in this work: (i) conventional secondary or tertiary low salinity waterfloods (LSW) where the injection brine is changed to increasingly ilute brines (either secondary: FB → LS or tertiary: FB → SW → LS) and (ii) inverted secondary or tertiary inverse

waterfloods (iLSW) where the injection brine sequence is reversed, and increasingly concentrated brines are injected (secondary: LS → FB or tertiary: LS → SW → FB). In all corefloods, the samples were aged in the first injection brine.

We begin by reporting coreflood results from conventional LSW. Our earlier results and other published results (e.g. 11,12) show that LSW yields a more negative zeta potential at the mineral-brine interface (Figure 3). Figure 11 reports examples of conventional LSW in both secondary and tertiary mode; additional LSW coreflood results are available in the Supplementary Material.

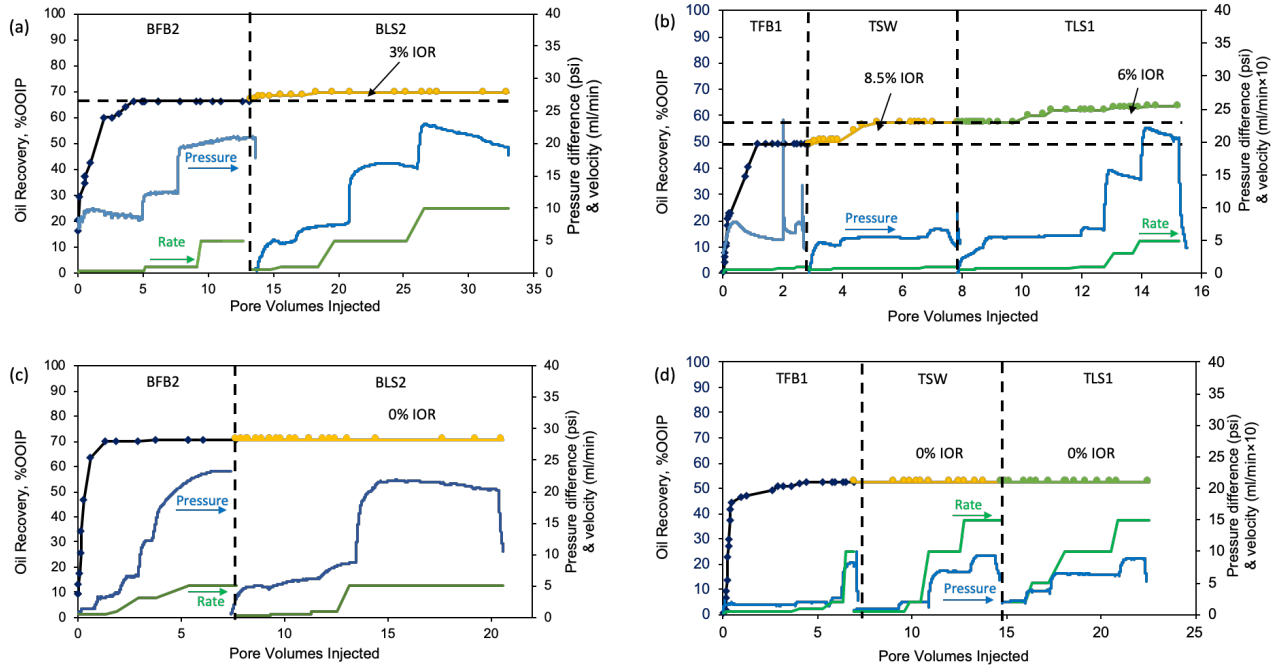

Figure 11 - Examples of conventional LSW corefloods. Plots (a) and (b) show typical results using crude-oils, Oil BM and Oil TT respectively, interpreted to have a negative oil-brine zeta potential in the aging brine; plots (c) and (d) show typical results using crude-oils, Oil BD and Oil TT respectively, interpreted to have a positve oil-brine zeta potential. Results shown correspond to (a) experiment 19 in Table 2; (b) experiment 21 in Table 2; (c) experiment 12 in Table 2 and (d) experiment 20 in Table 2. All corefloods shown here were performed at laboratory temperature. Additional LSW coreflooding results for the experiments listed in Table 2 can be found in the supplementary data.

In all of the LSW corefloods conducted to date, crude oils that were interpreted to have a negative zeta potential showed an increase in oil recovery (IOR) (e.g. Figure 11 (a) and (b)) whereas oils that were inferred to have a positive zeta potential showed no IOR (e.g. Figure 11 (c) and (d)). These trends were observed regardless of the specific brines, coreflooding mode and temperature. A notable result is for Oil BD, which was interpreted to have a positive zeta potential at laboratory conditions but a negative zeta potential at elevated temperature. The LSW at laboratory temperature showed no IOR, whereas at elevated temperature, LSW yielded an additional recovery of 2.2% (Figure 12).

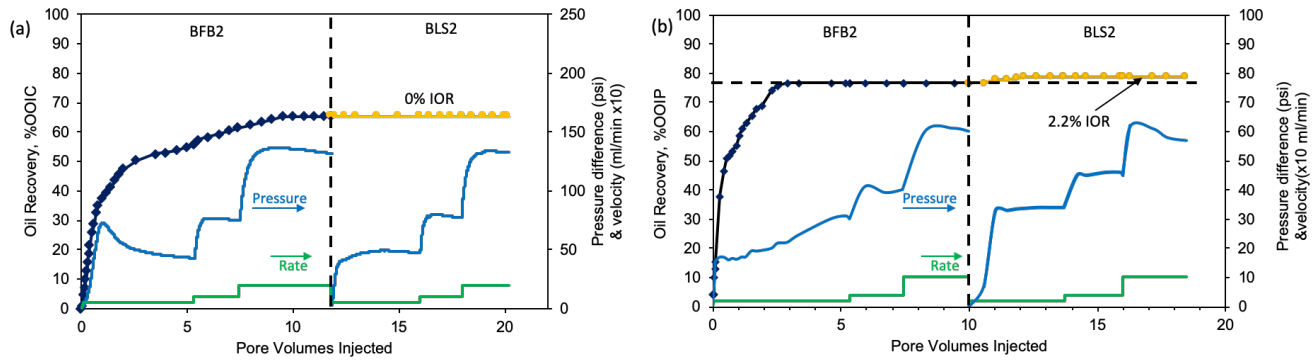

Figure 12 - Conventional LSW in sample BD saturated with oil BD at (a) ambient temperature where the zeta potential of the oil-brine interface was determined to be positive (Experiment 11 in Table 2) and (b) at elevated temperature where the zeta potential of the oil-brine interface was determined to be negative (Experiment 16 in Table 2).

Figure 13 reports examples of inverse iLSW in both secondary and tertiary mode; additional iLSW coreflood results are available in the Supplementary Material

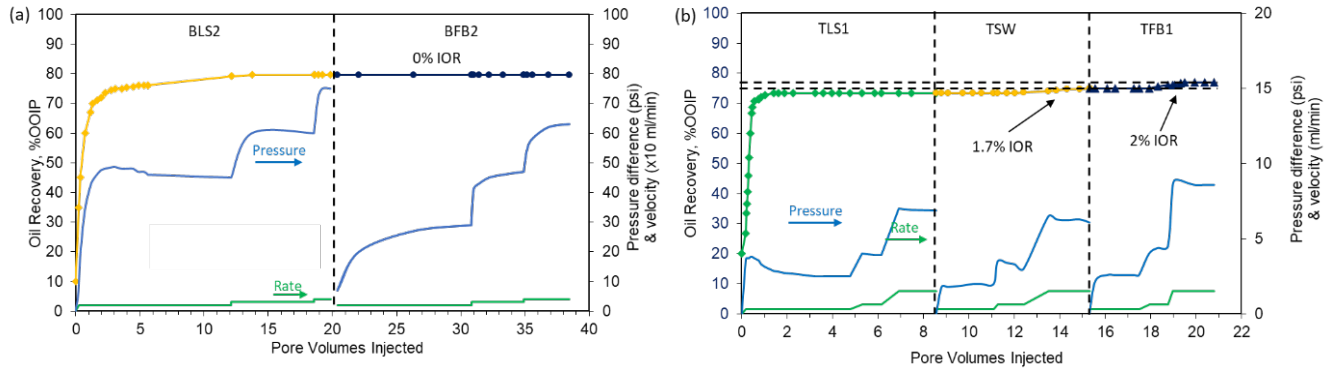

Figure 13 – Examples of conventional iLSW corefloods. Plot (a) shows a typical result using crude-oils BD interpreted to have a negative oil-brine zeta potential in the aging brine (Experiment 15 in Table 2); plot (b) shows typical results using crude-oil TT interpreted to have a positive oil-brine zeta potential (Experiment 22 in Table 2). Plot (a) was performed at elevated temperature whilst plot (b) was performed at ambient temperature. Additional iLSW coreflooding results for the experiments listed in Table 2 can be found in the supplementary data.

In the iLSW, crude oils interpreted to have a negative oil-brine zeta potential interface showed no IOR (e.g. Figure 13 (a)) whereas crude oils interpreted to have a positive oil-brine zeta potential typically showed IOR (e.g. Figure 13 (b)). The one exception was an iLSW with crude oil TT in sample TR (Figure 14). However, as discussed previously, the interpreted zeta potential for the crude oil was ambiguous, as the sample zeta potential was negative and became more positive (but was still negative) after aging (Figure 9). Hence, in this case, it seems likely that the polarity of the oil-brine zeta potential was incorrectly interpreted and is in fact negative.

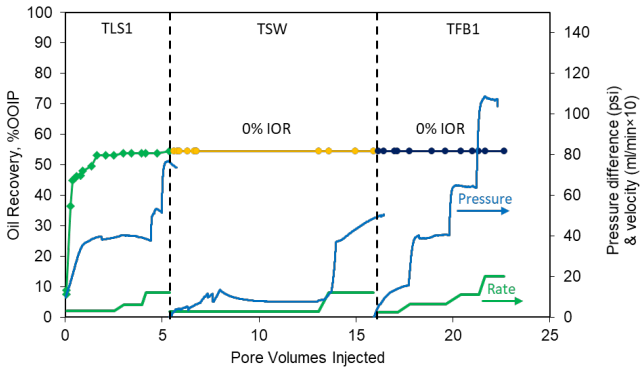

Figure 14 – iLSW coreflood with crude oil TT in sample TR performed at ambient temperature (Experiment 23 in Table 2). The zeta potential became more positive after aging but did not yield an IOR response unlike other iLSW where the zeta potential became more positive after aging.

Crude oil BD was interpreted to have a positive oil-brine zeta potential after aging in formation brine in sample BH at elevated temperature (Figure 7) and showed no IOR in a conventional LSW (Figure 15a), consistent with the other results reported here and by [9]. The sample was then cleaned and aged in low salinity brine in the same sample, after which it was interpreted to have a

negative oil-brine zeta potential (Figure 9). An iLSW coreflood was then conducted but no IOR was observed (Figure 15b), again consistent with the other results reported here and by [9]. Regardless of flooding sequence, no IOR was observed during CSW for crude oil BD in sample BH. The interpretation of the oil-brine zeta potential in both instances was unambiguous.

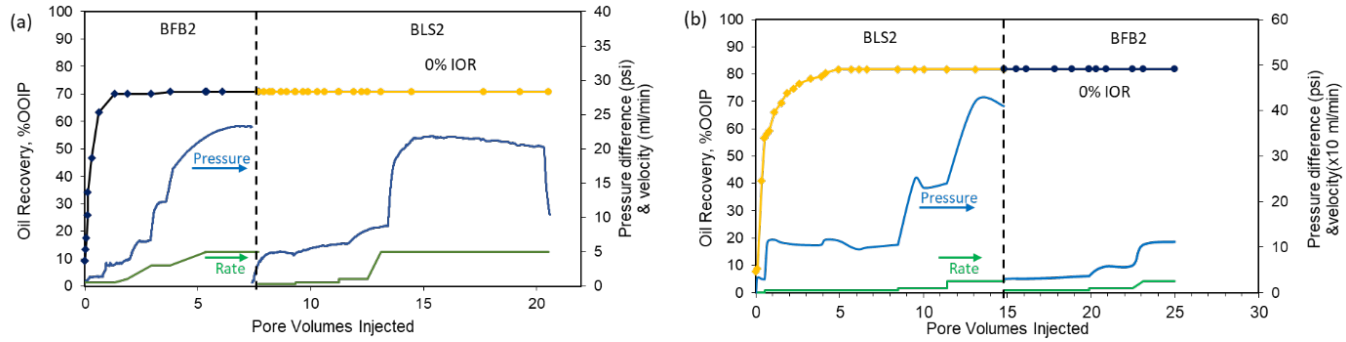

Figure 15 – CSW using crude oil BD in sample BH. Plot (a) shows a conventional LSW (experiment 12 in Table 2); plot (b) shows an iLSW (Experiment 13 in Table 2). Corefloods were performed at elevated temperature.

For a given coreflood sequence and COBR system we define a 'normalised zeta potential' given by:

$$\zeta_n = \left| \frac{\Delta\zeta_{CSW}}{\Delta\zeta_{wett} * I_w} \right| \qquad (4a)$$

$$\Delta\zeta_{CSW} = \zeta^{Injection\ Brine} - \zeta^{Aging\ Brine} \qquad (4b)$$

where $\Delta\zeta_{CSW}$ is the change in the mineral-brine zeta potential caused by injection of a CSW brine, determined from single-phase measurements (e.g. Figure 3). Equation (4) is empirical, modified from the expression suggested by Jackson et al. [9] to account for the initial wetting state as quantified by the value of I_w in the denominator. Jackson et al. [9] only used one core type and I_w was largely constant in their experiments. Here, we include I_w to account for the observation that

IOR during CSW depends in part on the initial wetting state, with more oil-wet samples having a greater potential for IOR [2-9, 22, 34, 38, 41, 42]. For successful CSW corefloods that yield IOR, we plot IOR (%) against ζ_n, (Figure 16), where we observe a correlation between IOR and normalised zeta potential regardless of the core type, crude oil, brine compositions, temperature or flooding sequence. Ambient temperature corefloods are given by triangular symbols and elevated temperature corefloods are shown by circular symbols.

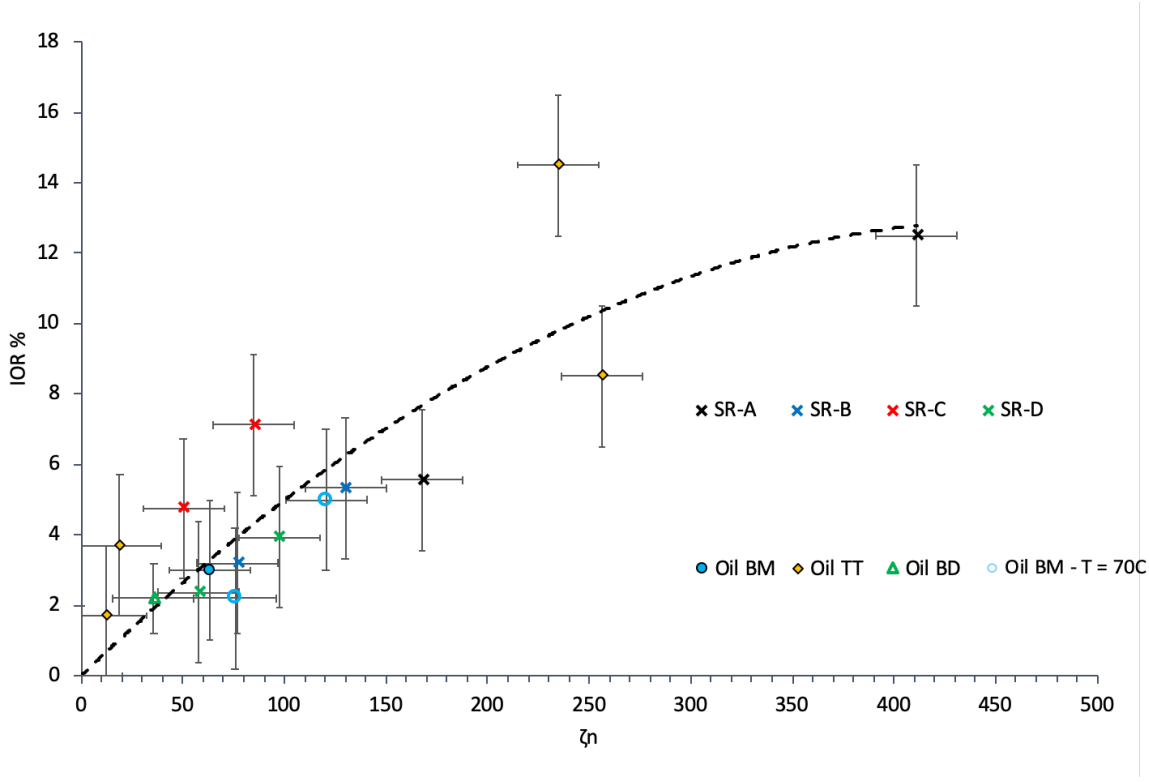

Figure 16 - Incremental oil recovered from successful CSW as a function of normalised zeta potential. Filled symbols represent data obtained at ambient temperature. Open symbols represent data obtained at elevated temperature. Data for oils SR-A to SR-D previously reported [9] and shown by crosses.

Discussion

Based on the suite of single and multiphase corefloods we have conducted to date, combining the new dataset obtained here with that reported by [9], we can compile the following observations:

- Dilution of the injection brine yields a more negative mineral-brine zeta potential regardless of sample type or temperature for realistic formation and dilute brine compositions.

- All conventional LSW corefloods have shown an IOR response when the crude oil is interpreted to have a negative oil-brine zeta potential in the aging brine.

- All bar one iLSW corefloods have shown an IOR response when the crude oil is interpreted to have a positive oil-brine zeta potential in the aging brine. Interpretation of the oil-brine zeta potential was ambiguous in the one exception and it is possible that it was negative, in which case the results are consistent with all other samples reported here.

- No IOR has been observed in any coreflood when the change in polarity of the mineral-brine zeta potential was opposite to that of the interpreted polarity of the oil-brine zeta potential in the aging brine.

- The effect of temperature on the success of LSW is directly linked to the effect of temperature on the zeta potential at the mineral-brine and oil-brine interfaces, such that the observations above are honoured.

- IOR during CSW can be correlated with a normalized change in zeta potential that accounts for the change in mineral-brine zeta potential in response to changing brine composition, the interpreted oil-brine zeta potential (represented by the change in zeta potential in response to aging in the crude oil) and the Amott water-wetting index.

615 Inclusion of I_w in the empirical expression for normalized zeta potential (4) accounts for
616 the observed link between initial wetting state and IOR during CSW.
617
618 • The results and key observations for IOR during CSW reported here are consistent with
619 those of Jackson et al. [9] (see Table 2 for a summary) and provide further support for the
620 Jackson et al. [9] model for CSW, in which the change in brine composition must be
621 chosen such that it yields an increased electrostatic repulsion between the mineral-brine
622 and oil-brine interfaces, and that the polarity of the zeta potential at the oil-brine interface
623 must also be determined in addition to the polarity of the mineral-brine interface. It is
624 incorrect to assume the zeta potential of the oil-brine interface is always negative, and
625 LSW failures observed previously may have been caused by a positive oil-brine zeta
626 potential that had not been recognized.
627
628 **Table 2** - Summary of all CSW carbonate corefloods to date reporting the polarity of the oil interpreted from the
629 change in zeta potential after aging, whether IOR was observed, and if these observations fit with the CSW model of
630 Jackson et al., [9]. 1-6 previously reported by [9]. Experiments marked with (*) represent experiments where there may
631 be a potential ambiguity in the interpretation of the oil-brine zeta potential polarity.
632

Number	Sample	Oil	CSW type	Conditions	Interpreted Oil-Brine Zeta-Potential Polarity	IOR Observed?	Consistent with Model?
1	Estaillades	SR-A	Normal	Ambient	+	No	Yes
2	Estaillades	SR-A	Inverse	Ambient	+ (*)	Yes	Yes (*)
3	Estaillades	SR-B	Normal	Ambient	-	Yes	Yes
4	Estaillades	SR-C	Normal	Ambient	-	Yes	Yes
5	Estaillades	SR-D	Normal	Ambient	-	Yes	Yes

6	Estaillades	SR-D	Inverse	Ambient	-	(*)	No	Yes (*)
7	BA	BD	Normal	Ambient	+		No	Yes
8	BB	BD	Normal	Ambient	+		No	Yes
9	BC	BD	Normal	Ambient	+		No	Yes
10	BF	BD	Normal	Ambient	+		No	Yes
11	BD	BD	Normal	Ambient	+		No	Yes
12	BH	BD	Normal	80	+		No	Yes
13	BH	BD	Inverse	80	-		No	Yes
14	BD	BD	Inverse	80	-		No	Yes
15	BD	BD	Inverse	80	-		No	Yes
16	BD	BD	Normal	80	-		Yes	Yes
17	BC	BM	Normal	80	-	(*)	Yes	Yes (*)
18	BC	BM	Normal	80	-	(*)	Yes	Yes (*)
19	BG	BM	Normal	Ambient	-	(*)	Yes	Yes (*)
20	TE	TT	Normal	Ambient	+		No	Yes
21	TR	TT	Normal	Ambient	-		Yes	Yes
22	TE	TT	Inverse	Ambient	+	(*)	Yes	Yes (*)
23	TR	TT	Inverse	Ambient	+	(*)	No	No (*)

Jackson et al., [9] assumed that the interpreted polarity of the oil-brine zeta potential was an intrinsic property of the crude oil and remained constant during CSW under reservoir relevant conditions. Here we see evidence of variation in the oil brine zeta potential polarity dependent on the brine composition, temperature and, interestingly in some cases, the core sample used, suggesting this previous assumption is invalid. However, there is further ambiguity in the interpretation of the oil-brine interface polarity in some instances via the method used here. Experiment 23, the iLSW with sample TR and Oil TT, is the only experiment that does not fit with the model of [9] based on the simple interpretation that the change in the zeta potential after aging is indicative of the oil-brine interface polarity used previously. However, if it is instead assumed that the zeta potential of this oil is negative, but less negative than the mineral surface,

644 this would yield the interpreted positive oil-brine zeta potential but the electrostatic model
645 controlling IOR by CSW is still valid and successful in explaining the lack of observed IOR. The
646 key discrepancy between the results presented here and those of Jackson et al., [9] lie within the
647 interpretation of the oil-brine interface. The method used here is not a direct measurement of the
648 oil-brine zeta potential. The zeta streaming potential method probes the mineral-brine interface
649 where the core is water wet and the oil-brine interface where the core is oil wet. This therefore
650 allows for an interpretation of the polarity of the oil-brine interface but not an accurate
651 measurement of the magnitude.
652
653 Published zeta potential measurements of the crude oil-brine interface are limited, although have
654 seen a recent increase as experimental techniques have improved and interest in the oil-brine zeta
655 potential for applications to CSW has increased [16, 23, 24, 26]. The majority of the measurements
656 are made using zetasizers or other commercially available equipment. As with the carbonate-brine
657 interface, these methods have a limited range of operating conditions that differ significantly from
658 natural oil reservoirs and make relevant measurements difficult to obtain. Measurements of the
659 oil-brine zeta potential are particularly challenging at reservoir conditions using high ionic strength
660 brines (>0.1M) and high temperature (>60°C), due to the difficulty in maintaining a stable
661 dispersion of oil droplets in brine long enough to record a measurement and the rapid degradation
662 of the electrodes.
663
664 Almost all of the published data of the oil-brine interface zeta potential report negative values at
665 pH >5, typical of carbonate reservoir pH's (pH 6-9, Figure 3), and become increasingly more
666 negative with increasing pH [33]. Most of the values are measured on oil droplet suspensions
667 within simple, single salt species electrolytes up to 0.1M ionic strength (commonly, NaCl, KCl,
668 $CaCl_2$ and $MgCl_2$) and the zeta potential typically decreases in magnitude with an increase in ionic
669 strength of the brine for a given pH ([23, 33-37]), consistent with conventional double-layer theory

[10]. Some studies report zeta potential measurements made in suspensions of multi-salt electrolytes or reservoir relevant seawaters or low salinity brines [4, 23, 24, 34, 38]. These are also always negative at the pH of interest and increase in magnitude with decreasing ionic strength and increasing pH. Despite the difficulties in obtaining data at conditions relevant to oil reservoirs, Mahani et al., do report a small but negative oil-brine zeta potential made in a zetasizer in a formation brine, however, this is only done at room temperature and not reservoir conditions and they do note the difficulty in maintaining a stable dispersion, especially at high and low pH values [4]. Experimental evidence for a positively charged oil-brine zeta potential does exist at low pH values [33, 37, 38]. The iso-electric point (IEP) is the pH at which the zeta potential switches from positive to negative and is typically around pH 3-5 for most of the published data but varies with the specific oil used. It has been suggested that the amounts of the organic acid and base components in the crude oil (given by the acid number, AN, and base number, BN) can be important in determining the IEP and the overall charge at the interface [24, 33, 37]. Crude oils with a higher AN/BN ratio typically show a lower IEP and more negatively charged oil-brine zeta potential values, however many studies suggest that the AN and BN are insufficient to accurately describe the properties and behaviour of the oil-brine interface, a recent study by Bonto et al., [36] suggested that these bulk properties of the crude-oils may not accurately represent the amounts of these species active at the oil-brine. Other evidence of positively charged crude oils also exists in high Ca^{2+} concentration electrolytes. Nasralla et al., [34] report a positive oil-brine zeta potential in a 50,000ppm $CaCl_2$ electrolyte but at a pH of 4, whilst Pooryousefy et al., report a positive oil-brine interface zeta potential also in 50,000ppm $CaCl_2$ at a pH of 7 [25]. This is a comparable Ca^{2+} concentration and brine pH to the formation brines used here in this work (Table 1) and, to the best of our knowledge, is the only positive oil-brine zeta potential observed above pH 6.

Brady et al., [39, 40] proposed a surface complexation model (SCM) for the crude oil-brine interface and suggest that the primary control on the interfacial charge is the protonation and

deprotonation reactions of the organic acid and base compounds of the crude oil, given by equations (5) & (6) respectively:

$$-COOH \leftrightarrow -COO^- + H^+ \qquad \text{LogK (25 °C) = -5.0} \quad (5)\ [39]$$

$$-NH^+ \leftrightarrow -N + H^+ \qquad \text{LogK (25 °C) = -6.0} \quad (6)\ [39]$$

At reservoir pH, these equations predict the majority of the basic groups will be neutrally charged and the acidic groups negatively charged yielding an overall negative charge at the interface which increases with increasing pH, but for pH values less than 5 there may be an overall net positive charge, consistent with experimental data. These equations also account for the apparent trend between the AN/BN ratio and the IEP. However Brady et al., [39, 40] and more recently Bonto et al., further suggested that other reactions between the acid and base groups in the oil and the ionic species in the brine (e.g. Na^+, Ca^{2+}, Mg^{2+}….) analogous to those of the carbonate-brine interface, could modify the polarity of the crude oil-brine interface to account for the positive charged observed in concentrated multivalent ion electrolytes, e.g:

$$-COOH + Na^+ \leftrightarrow COONa + H^+ \qquad \text{LogK (25 °C) = -4.86} \quad (7)\ [36]$$

$$-COOH + Ca^{2+} \leftrightarrow -COOCa^+ + H^+ \qquad \text{LogK (25 °C) = -3.8} \quad (8)\ [36]$$

$$-COOH + Mg^{2+} \leftrightarrow -COOMg^+ + H^+ \qquad \text{LogK (25 °C) = -3.5} \quad (9)\ [36]$$

These SCMs support the hypothesis for the potential of a positively charged crude oil-brine interface under certain conditions (low pH, high multivalent ion concentration…) typical of reservoir formation brines, at higher values of pH than previously reported, and at conditions not typically investigated by experimental studies. The most recent and advanced SCM for the oil-brine interface by Bonto et al., [36] proposed three different models of increasing complexity

721 which were successful in modelling a wide range of zeta potential data, but none were consistently
722 successful and definitive in modelling data across multiple experimental studies. Additionally, the
723 models predicted strongly positive zeta potential values in high concentration $CaCl_2$ and $MgCl_2$
724 brines that were inconsistent with the experimental data. They concluded that the key issues with
725 the models surrounded accurately describing the number of active polar species at the interface
726 and poor-quality reporting of the pH from experimental data. SCMs often contain parameters that
727 are tuned to match experimental data or obtained from experimental work, e.g. the LogK values
728 in equations 5-9 used by [36, 39], but this is obtained under ideal, laboratory conditions making
729 extrapolation to high ionic strength electrolytes or high temperatures relevant to oil reservoirs
730 questionable. Bonto et al., note their models perform worse in high ionic strength electrolytes
731 where experimental data is sparse and theoretical models are restricted [36].
732
733 Clearly, the current understanding of the oil-brine interface is insufficient for applications to true
734 reservoir conditions. No clear trends between the oil, brine or mineral properties and the
735 interpreted polarity of the oil-brine interface have been identified from our results that would allow
736 a prediction of the oil-brine polarity prior to conducting the experimental procedure. It is unclear
737 why Oil TT would exhibit both a positive and negative polarity dependent upon the core sample
738 type when aged in compositionally similar cores with the same brine (Figure 7). The effect of aging
739 on the oil-brine zeta potential also needs further investigation. Wettability alteration during aging
740 is acknowledged to occur due to chemical reactions between the COBR components (e.g. [7, 8,
741 33, 41, 42]) but the impact of this on the crude oil interfacial chemistry, and thus the zeta potential
742 is unclear. Additional modelling, and experimental data to constrain and validate those models, is
743 required at conditions relevant to oil reservoirs. The methodology used here is advantageous in
744 interpreting the polarity of the oil-brine zeta potential at reservoir conditions and correlating this
745 to IOR, but has possible ambiguities in the interpretation, cannot provide an accurate estimate of
746 the magnitude of the oil-brine zeta potential and is too time consuming and resource intensive to

747 systematically study the impact of individual variables on the interpreted polarity. Independent
748 experimental methods that can accurately measure the zeta potential of the oil-brine interface
749 under reservoir relevant conditions are necessary to systematically probe the impact of brine
750 composition and concentration, temperature and oil properties on the zeta potential to better
751 understand the behaviour of the interface and to predict and understand IOR by CSW.
752
753 ## Conclusions
754 1. It is important to determine how the relevant formation and injection brines used in CSW
755 will modify the zeta potential of both the mineral-brine and oil-brine interfaces at reservoir
756 conditions on intact samples.
757
758 2. The injection brine composition should be designed to yield a change in the mineral-brine
759 zeta potential that is of the same polarity as the crude oil-brine interface polarity in order
760 to increase oil recovery.
761
762 3. This change results in an increased electrostatic repulsion between the mineral-brine and
763 oil-brine interfaces, acting to increase the stability of a thin water film acting between the
764 two interfaces, resulting in a change towards a more water-wet core which is consistent
765 with the majority of literature observations of CSW. The change in the electrostatic forces,
766 not the total salinity, is more important for the success of CSW.
767
768 4. The crude oil-brine interface polarity of importance to CSW is that present after aging with
769 the formation brine and rock core of interest, not the pristine crude oil-brine interface.
770 The polarity of the crude oil-brine interface can vary depending upon the aging conditions
771 used. No correlation between the oil/brine/rock properties and the polarity of the crude

oil-brine interface inferred after aging have yet been identified. As such, there is currently no model to predict the crude oil-brine interface polarity of a given COBR system prior to measuring experimentally.

5. The polarity of the crude oil-brine interface is unlikely to be constant during CSW. It is currently unknown if, or how, modifying the injection brine composition may alter this. Additional data and models are required to increase our understanding.

Acknowledgements

The authors acknowledge and thank BP Exploration and TOTAL for providing funding and samples used in this paper and for granting permission to publish.

Conflict of Interests

The authors declare no conflicts of interest.

References:

1. Klemme, H. and G.F. Ulmishek, *Effective petroleum source rocks of the world: stratigraphic distribution and controlling depositional factors (1).* AAPG Bulletin, 1991. **75**(12): p. 1809-1851.
2. Yousef, A.A., et al., *Laboratory Investigation of the Impact of Injection-Water Salinity and Ionic Content on Oil Recovery From Carbonate Reservoirs.* SPE Reservoir Evaluation & Engineering, 2011. **14**(05): p. 578-593.
3. Austad, T., et al., *Conditions for a Low-Salinity Enhanced Oil Recovery (EOR) Effect in Carbonate Oil Reservoirs.* Energy & Fuels, 2012. **26**(1): p. 569-575.

4. Mahani, H., et al., *Insights into the Mechanism of Wettability Alteration by Low-Salinity Flooding (LSF) in Carbonates.* Energy & Fuels, 2015. **29**(3): p. 1352-1367.
5. Fathi, S.J., T. Austad, and S. Strand, *"Smart Water" as a Wettability Modifier in Chalk: The Effect of Salinity and Ionic Composition.* Energy & Fuels, 2010. **24**(4): p. 2514-2519.
6. Gandomkar, A. and M.R. Rahimpour, *Investigation of Low-Salinity Waterflooding in Secondary and Tertiary Enhanced Oil Recovery in Limestone Reservoirs.* Energy & Fuels, 2015. **29**(12): p. 7781-7792.
7. Hiorth, A., L. Cathles, and M. Madland, *The impact of pore water chemistry on carbonate surface charge and oil wettability.* Transport in porous media, 2010. **85**(1): p. 1-21.
8. Zhang, P. and T. Austad, *Wettability and oil recovery from carbonates: Effects of temperature and potential determining ions.* Colloids and Surfaces A: Physicochemical and Engineering Aspects, 2006. **279**(1): p. 179-187.
9. Jackson, M.D., D. Al-Mahrouqi, and J. Vinogradov, *Zeta potential in oil-water-carbonate systems and its impact on oil recovery during controlled salinity water-flooding.* Sci Rep, 2016. **6**: p. 37363.
10. Hunter, R.J., *Zeta potential in colloid science : principles and applications*. 1981, London: Academic Press.
11. Al Mahrouqi, D., J. Vinogradov, and M.D. Jackson, *Zeta potential of artificial and natural calcite in aqueous solution.* Adv Colloid Interface Sci, 2017. **240**: p. 60-76.
12. Alroudhan, A., J. Vinogradov, and M.D. Jackson, *Zeta potential of intact natural limestone: Impact of potential-determining ions Ca, Mg and SO4.* Colloids and Surfaces A: Physicochemical and Engineering Aspects, 2016. **493**: p. 83-98.

13. Foxall, T., et al., *Charge determination at calcium salt/aqueous solution interface.* Journal of the Chemical Society, Faraday Transactions 1: Physical Chemistry in Condensed Phases, 1979. **75**: p. 1034-1039.
14. Alotaibi, M.B., et al., *Dynamic interactions of inorganic species at carbonate/brine interfaces: An electrokinetic study.* Colloids and Surfaces A: Physicochemical and Engineering Aspects, 2018. **550**: p. 222-235.
15. Alotaibi, M.B. and A.A. Yousef, *The Role of Individual and Combined Ions in Waterflooding Carbonate Reservoirs: Electrokinetic Study.* Spe Reservoir Evaluation & Engineering, 2017. **20**(1): p. 77-86.
16. Mahani, H., et al., *Electrokinetics of Carbonate/Brine Interface in Low-Salinity Waterflooding: Effect of Brine Salinity, Composition, Rock Type, and pH on zeta-Potential and a Surface-Complexation Model.* Spe Journal, 2017. **22**(1): p. 53-68.
17. Song, J., et al., *Surface complexation modeling of calcite zeta potential measurements in brines with mixed potential determining ions (Ca2+, CO32−, Mg2+, SO42−) for characterizing carbonate wettability.* Journal of Colloid and Interface Science, 2017. **506**: p. 169-179.
18. Chen, L., et al., *Zeta potential of limestone in a large range of salinity.* Colloids and Surfaces A: Physicochemical and Engineering Aspects, 2014. **450**: p. 1-8.
19. Kasha, A., et al., *Effect of Ca2+, Mg2+ and SO42− ions on the zeta potential of calcite and dolomite particles aged with stearic acid.* Colloids and Surfaces A: Physicochemical and Engineering Aspects, 2015. **482**: p. 290-299.
20. Awolayo, A., H. Sarma, and A. AlSumaiti, *An Experimental Investigation into the Impact of Sulfate Ions in Smart Water to Improve Oil Recovery in Carbonate Reservoirs.* Transport in Porous Media, 2016. **111**(3): p. 649-668.

21. Fathi, S.J., T. Austad, and S. Strand, *Water-Based Enhanced Oil Recovery (EOR) by "Smart Water": Optimal Ionic Composition for EOR in Carbonates.* Energy & Fuels, 2011. **25**(11): p. 5173-5179.

22. Nasralla, R.A., M.A. Bataweel, and H.A. Nasr-El-Din, *Investigation of Wettability Alteration by Low Salinity Water*, in *Offshore Europe*. 2011, Society of Petroleum Engineers: Aberdeen, UK.

23. Takeya, M., et al., *Predicting the electrokinetic properties of the crude oil/brine interface for enhanced oil recovery in low salinity water flooding.* Fuel, 2019. **235**: p. 822-831.

24. Takeya, M., et al., *Effect of acid number on the electrokinetic properties of crude oil during low salinity waterflooding.* Energy & Fuels, 2019.

25. Pooryousefy, E., et al., *Drivers of low salinity effect in sandstone reservoirs.* Journal of Molecular Liquids, 2018. **250**: p. 396-403.

26. Nazarova, M., P. Bouriat, and P. Creux, *Electrical Double-Layer Expansion Impact on the Oil–Quartz Adhesion for High- and Low-Salinity Brines.* Energy & Fuels, 2018. **32**(7): p. 7319-7325.

27. Al Mahrouqi, D., J. Vinogradov, and M.D. Jackson, *Temperature dependence of the zeta potential in intact natural carbonates.* Geophysical Research Letters, 2016. **43**(22): p. 11,578-11,587.

28. Jackson, M.D. and J. Vinogradov, *Impact of wettability on laboratory measurements of streaming potential in carbonates.* Colloids and Surfaces A: Physicochemical and Engineering Aspects, 2012. **393**: p. 86-95.

29. Vinogradov, J., M.Z. Jaafar, and M.D. Jackson, *Measurement of streaming potential coupling coefficient in sandstones saturated with natural and artificial brines at high salinity.* Journal of Geophysical Research, 2010. **115**(B12).

30. Vinogradov, J. and M.D. Jackson, *Zeta potential in intact natural sandstones at elevated temperatures.* Geophysical Research Letters, 2015. **42**(15): p. 6287-6294.

31. Li, S., et al., *Influence of surface conductivity on the apparent zeta potential of calcite.* Journal of Colloid and Interface Science, 2016. **468**: p. 262-275.

32. Jackson, M.D., et al., *Spontaneous Potentials in Hydrocarbon Reservoirs During Waterflooding: Application to Water-Front Monitoring.* 2012.

33. Buckley, J.S., K. Takamura, and N.R. Morrow, *Influence of Electrical Surface Charges on the Wetting Properties of Crude Oils.* SPE Reservoir Engineering, 1989. **4**(03): p. 332-340.

34. Nasralla, R.A. and H.A. Nasr-El-Din, *Double-Layer Expansion: Is It A Primary Mechanism of Improved Oil Recovery by Low-Salinity Waterflooding?*, in *SPE Improved Oil Recovery Symposium*. 2012, Society of Petroleum Engineers: Tulsa, Oklahoma, USA.

35. Ayirala, S.C., et al., *Coalescence of Crude Oil Droplets in Brine Systems: Effect of Individual Electrolytes.* Energy & Fuels, 2018. **32**(5): p. 5763-5771.

36. Bonto, M., A.A. Eftekhari, and H.M. Nick, *An overview of the oil-brine interfacial behavior and a new surface complexation model.* Scientific Reports, 2019. **9**(1): p. 6072.

37. Kolltveit, Y., *Relationship Between Crude Oil Composition and Physical-Chemical Properties*, in *Department of Chemistry*. 2016, University of Bergen.

38. Alshakhs, M.J. and A.R. Kovscek, *Understanding the role of brine ionic composition on oil recovery by assessment of wettability from colloidal forces.* Advances in Colloid and Interface Science, 2016. **233**: p. 126-138.

39. Brady, P.V., et al., *Electrostatics and the Low Salinity Effect in Sandstone Reservoirs.* Energy & Fuels, 2015. **29**(2): p. 666-677.

40. Brady, P.V. and J.L. Krumhansl, *A surface complexation model of oil–brine–sandstone interfaces at 100°C: Low salinity waterflooding.* Journal of Petroleum Science and Engineering, 2012. **81**: p. 171-176.

41. Buckley, J.S., Y. Liu, and S. Monsterleet, *Mechanisms of Wetting Alteration by Crude Oils.* 1998.

42. Drummond, C. and J. Israelachvili, *Fundamental studies of crude oil–surface water interactions and its relationship to reservoir wettability.* Journal of Petroleum Science and Engineering, 2004. **45**(1): p. 61-81.

43. Fuerstenau, D. W., *Measuring zeta potentials by streaming potential techniques*. Trans. AIME, 1956, 205, 834-835.

44. Jackson, M. D. (2010), Multiphase electrokinetic coupling: Insights into the impact of fluid and charge distribution at the pore scale from a bundle of capillary tubes model, *J. Geophys. Res.*, 115, B07206, doi:10.1029/2009JB007092.

45. Jackson and Leinov, 2012, On the Validity of the “Thin” and “Thick” Double-Layer Assumptions When Calculating Streaming Currents in Porous Media, Int J. Geophysics, 897807, doi:10.1155/2012/897807).